Accessing Acute Care Hospitals in the San Francisco Bay after a Major Hayward Earthquake

Luis Ceferino[1,2,*], Charan Kukunoor[2], Dan Mao[3], Xinlu Xu[2], Jingzhe Wu[4], and Adam Zsarnóczay[5]

[1]Department of Civil and Environmental Engineering, University of California, Berkeley
[2]Department of Civil and Urban Engineering, New York University
[3]Center for Urban Science and Progress, New York University
[4]The Global Facility for Disaster Risk Reduction, the World Bank Group
[5]Department of Civil and Environmental Engineering, Stanford University
[*]Corresponding author. Mailing address: 773 Davis Hall, Berkeley, CA 94720, USA. Email: ceferino@berkeley.edu

Abstract

Earthquakes can severely disrupt healthcare services for many communities, especially in dense cities. Here, we study the acute care hospital system in San Francisco Bay, California, to identify the most impacted communities after a magnitude 7.25 earthquake on the Hayward Fault. We integrate seismic hazard information with unique granular infrastructure vulnerability and connectivity data for 76 acute care hospitals with 426 buildings and 16,639 beds. We leverage the rich data to formulate a coupled risk-network model that anticipates infrastructure failures and cascading effects affecting healthcare access. We show that the bed capacity within hospital buildings can be reduced to 49%. In East Bay, Alameda County will concentrate most losses, preserving only 19% of capacity. We also found that communities will travel disparately longer to access functioning hospitals, reshaping healthcare access across the entire Bay. The regional travel time will increase by 27%, but at micro-urban scales, increases are way higher and can be above 400% in East Bay. This study demonstrates the urgent need to prepare emergency plans and strengthen the healthcare infrastructure.

Earthquakes wield the power to disrupt healthcare access and affect many communities simultaneously, especially in densely populated regions.[1] For example, the recent M 7.8 earthquake in Turkey left tens of thousands without hospital services after damaging more than 50 hospitals.[2] In a mass-casualty earthquake,[3,4] several thousands of severely injured people can worsen their health, even up to deadly conditions, if they do not receive timely access to medical services, e.g., 2005 Pakistan, 2010 Haiti, 2008 China, 2011 Japan, 2023 Turkey.[5–10] These communities can lose healthcare access for many years.[11] For example, many communities lost access to their local critical medical services (e.g., dialysis) for up to five years after the 2003 Bam earthquake in Iran due to slow reconstruction.[12]

In the U.S., many communities have lost access to healthcare following previous earthquakes, even though earthquakes have only been moderate in magnitude. The 1971 M 6.6 San Fernando

Corresponding author: Luis Ceferino. E-mail: ceferino@berkeley.edu

Earthquake severely damaged four major hospitals, which had to be evacuated. Two hospital buildings collapsed, killing more than 40 people.[13] In response to this earthquake, the Alfred E. Alquist Hospital Seismic Safety Act was enacted in 1973 to create a new, resilient hospital infrastructure in California. The Legislature noted that "*hospitals, that house patients who have less than the capacity of normally healthy persons to protect themselves, and that must be reasonably capable of providing services to the public after a disaster, shall be designed and constructed to resist, insofar as practical, the forces generated by earthquakes, gravity and winds.*"[13]

In 1994, the M 6.7 Northridge Earthquake disrupted 11 hospitals.[14] Eight acute care hospitals in Los Angeles County (9% of the total) had to be evacuated,[15] causing accumulated losses of USD 3 billion. Twelve Pre-Alquist Act hospital buildings received red tags after engineers considered them too dangerous for reentry. Post-Alquist Act hospital buildings experienced less structural damage, but non-structural damage was still extensive.[16] These large disruptions of healthcare services after the moderate Northridge Earthquake led to the California Senate Bill 1953. The Bill requires retrofitting a large part of the acute care infrastructure by 2030 to create a path to make existing buildings from acute care hospitals resilient.[17,18] Notably, many hospitals do not have the financial resources to comply with the ordinance and are unlikely to meet the deadline.[19]

In response to these high vulnerabilities, this paper investigates the effects of future earthquakes on healthcare access in the entire San Francisco Bay, California. Significant research efforts have been devoted to understanding and modeling disruptions to healthcare services after earthquakes but with a main focus on individual facilities. Some researchers focused on characterizing failures in healthcare infrastructure components using structural engineering, performance-based analyses, and fault trees.[20–23] These researchers model damage to structural and non-structural components of the infrastructure supporting healthcare services within buildings to evaluate the post-earthquake functionality of hospitals. Other researchers have focused on characterizing the dynamics of medical processes in an earthquake emergency, but also at the single-building scale.[24–27] They use discrete event simulations and flow models to assess patient waiting and treatment times, explicitly accounting for patient surges and the available medical resources after earthquakes.

However, hospitals do not behave as isolated units, especially in large cities. When an earthquake disrupts a hospital, network effects cascade the impacts to entire cities, e.g., earthquakes in Chile, New Zealand, and Japan.[21,28–31] Network effects propagate and exacerbate impacts in two fundamental ways. First, failures in a few hospitals can overload hospitals in the entire network, affecting communities within and beyond the damaged hospital's catchment area. Logically, people who lose their local hospital must travel longer to find healthcare services. Longer travel times result in a longer time to treatment, which can have drastic (and even lethal) consequences on the health of critically injured people, e.g., crush syndrome and cardiac arrest.[32–34] In addition, communities whose local hospitals do not fail will also wait longer for treatment since their functioning hospitals must receive patients from other communities in the city, especially those whose local hospitals failed. Second, failures in a few hospitals can also overload the healthcare network's supporting infrastructure, such as the transportation network.[35,36] More injured people will seek medical services in fewer hospitals, increasing traffic across the city, especially in emergency corridors, highways, and roads leading to the functioning hospitals. Because fewer hospitals are functional, the reliance on the supporting transportation infrastructure also increases. Thus, emergency responders must identify the key transportation links to ensure they work effectively after the earthquake and avoid significant delays in travel times for many patients. While these two cascading effects start during the emergency, they continue until the entire hospital infrastructure is recovered, in many

cases for years.[11,12]

Researchers have recently developed a few models for capturing these network effects in large regions. These models have been applied to different regions and hazards, e.g., earthquakes, hurricanes, wildfire, and pandemics.[11,37–39] These models vary in computational and formulation complexity. While these models can, in principle, be extended to any region, data scarcity becomes a fundamental problem, requiring different reformulating approaches to adjust to specific case studies.

This paper investigates failures and network effects on healthcare access in the Bay after earthquakes by carefully formulating a large-scale risk-network model that leverages granular and rich data from California's hospital infrastructure (see Methods). Investigating post-earthquake healthcare in the Bay addresses fundamental knowledge gaps in disaster emergency research because, unlike the past few studies on hospital networks,[11,37–39] we can focus on urban and diverse communities exposed to earthquakes only within a few kilometers from them. In addition, the rich Bay's infrastructure data provide this study with a unique testbed to analyze the disparate and granular effects of earthquakes on public health across urban communities. Thus, this study offers insights into post-earthquake healthcare access for many cities with diverse communities and vulnerable hospitals exposed to earthquakes within or near their geographical extents, e.g., cities in the U.S., Japan, and Turkey with active shallow seismic faults.

Our model to study California combines state-of-the-art disaster risk analysis with a simplified network model to cleanly study post-earthquake healthcare access with computational efficiency, allowing for assessing thousands of potential scenarios of earthquake disruption (see Methods). Our results leverage unique information with granular categorizations of structural and non-structural vulnerabilities of 76 acute care hospitals' 426 buildings to identify the facilities more likely to lose functionality after an M 7.25 earthquake on the Hayward Fault. This research serves as a first-cut assessment to help cities identify the communities with access to health services most significantly affected, considering the complex network effects in healthcare and supporting infrastructure within cities.

Results

The Bay is home to more than 7M people in Northern California, and as a major city, it has a large demand for healthcare. Seventy-six acute care hospitals provide the Bay's communities with inpatient medical care and other related services for surgery, acute medical conditions, or injuries (usually for a short-term illness or condition). These hospitals are critical for emergencies such as those after moderate and large earthquakes.

Much of the Bay's acute care infrastructure portfolio is exposed to extreme seismic hazards due to the proximity to seismic faults. Figure 1 shows that most hospitals are bounded by the San Andreas and the Hayward Fault, where major earthquakes (> 7.0) can occur. The Laguna Honda Hospital and Rehabilitation Center and the University of California, San Francisco (UCSF) Medical Center are the largest acute care hospitals, with 780 and 580 beds. Both are located in San Francisco, less than 2 km from each other, showing that medical resources can be concentrated in small regions in the Bay. The three zip codes with the most beds are Palo Alto, San Francisco (where the two largest hospitals are), and San Jose, with 1410, 1360, and 932 beds, respectively.

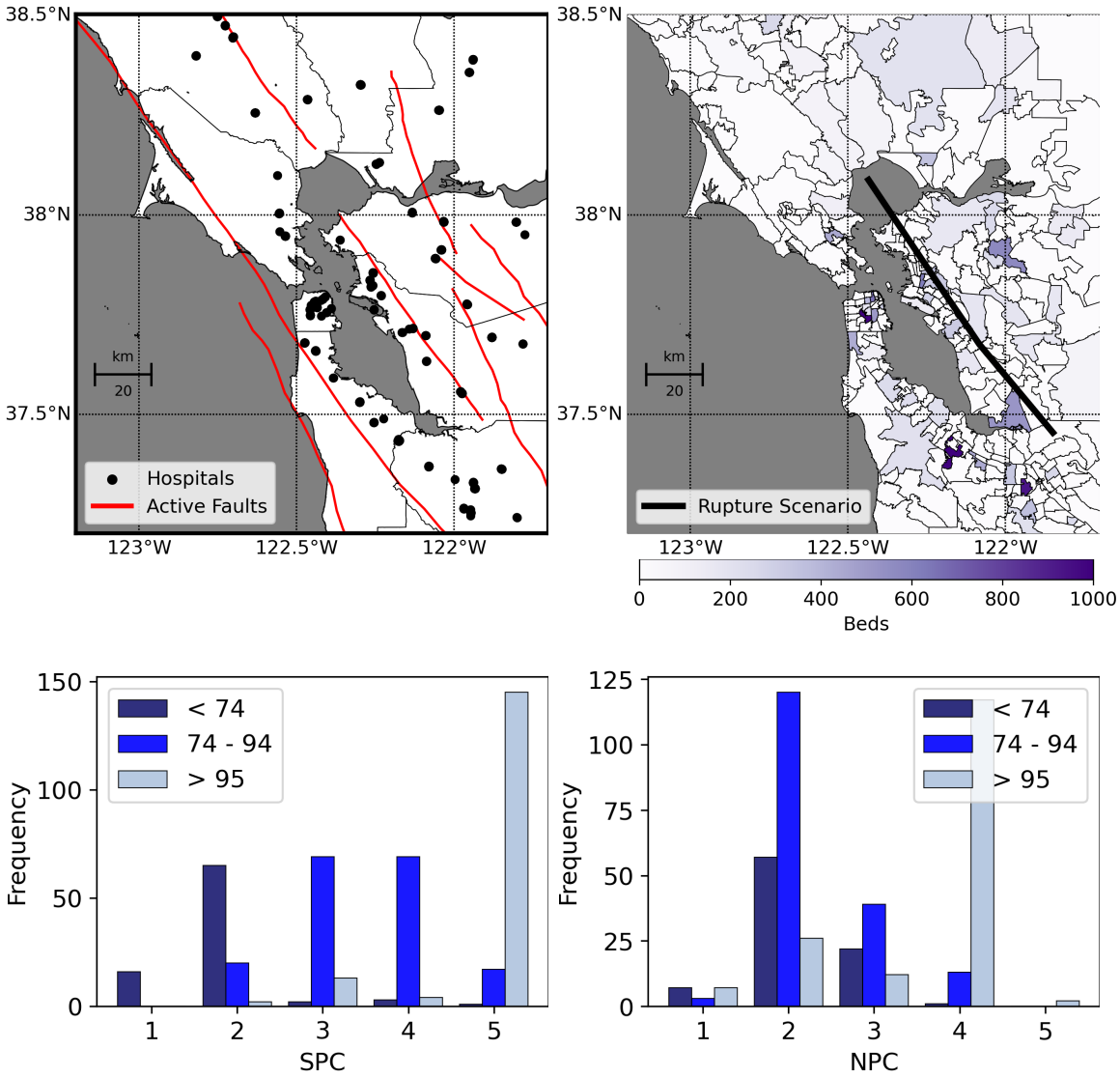

Figure 1: Seismic hazard and hospital exposure and vulnerability in the San Francisco Bay, California. Upper left: Acute care hospital inventory and all major active faults. Upper right: Bed count per zip code and M 7.25 rupture scenario on the Hayward Fault. Lower Left: Histogram of hospital buildings' structural performance category (SPC) and their years of construction. Lower right: Lower left: Histogram of hospital buildings' non-structural performance category (NPC) and their years of construction.

Acute Care Vulnerability in the San Francisco Bay

We found that a significant part of the acute care portfolio is seismically vulnerable due to structural or non-structural deficiencies (Figure 1). To quantify the extent of vulnerabilities, we compiled information from 426 buildings belonging to the 76 acute care hospitals in the Bay, including structural typologies, year of construction, number of stories, and seismic vulnerability ratings.[18,40,41] Supplementary Note 1 and Supplementary Figure 1 describe and summarize the hospitals' years of construction, structural typologies, and the number of stories. The Methods section establishes how to use this information to model seismic vulnerability, as these building features indicate

buildings' dynamic properties, strength, and ductility. Here, we describe the Structural Performance Categories (SPC) and Non-structural Performance Categories (NPC), established by California's Department of Health Care Access and Information (HCAI) to characterize structural and non-structural deficiencies.[42] Each hospital building receives vulnerability ratings (SPC or NPC) ranging from 1 to 5, from the most to the least vulnerable. Supplementary Tables 1 and 2 fully describe SPC and NPC.

Many buildings have high structural vulnerabilities (Figure 1). 16 (4%) hospital buildings have an SPC of 1. All of them were built before 1974 and have a high collapse probability for earthquakes that regular buildings designed with modern codes would withstand (i.e., earthquakes with a return period of 475 years).[43] None of these buildings were supposed to provide acute care services by 2020. 87 (20%) hospital buildings have an SPC of 2; 65 were built before 1974, and 20 between 1974 and 1994. They meet pre-1973 standards for regular buildings but not the standards for hospitals.[44] SPC-2 buildings need to be upgraded by 2030. Only SPC-3, SPC-4, and SPC-5 buildings can be used after 2030. SPC-5 buildings have the highest structural ratings and are equivalent to an essential facility in modern building standards,[43] i.e., these buildings have to be strong enough to be immediately occupiable after design earthquakes (return period of 475 years) and cannot threaten the occupants' lives even in maximum credible earthquakes (return period of 2,475 years).[43] 163 (38%) buildings are SPC-5, and 145 were built after 1994.

We found that non-structural vulnerabilities are even more widespread. 220 buildings (52%) have an NPC of two or below (Figure 1). 64 were built before 1974, and 123 between 1974 and 1994. NPC-2 buildings have proper anchorage and bracing only in a few non-structural components, mainly for building access. They should have had to be upgraded by 2002 to be operational for acute services. NPC-4 buildings have all their non-structural components properly anchored, and after 2030, all buildings should meet this standard. 131 buildings are NPC-4, and 117 were built after 1994. NPC-5 buildings have additional requirements for 72 hours of continuous hospital operations, but only 2 are in this category. Notice that a hospital building designed with modern codes[43] may fall below NPC-5 even if all non-structural components within the building are secured since on-site supplies for continuous acute care operations (e.g., water tanks) can be outside the building.

Earthquake Scenario and Projected Building Damage

We studied an earthquake scenario of M 7.25 on the Hayward Fault in East Bay (Figure 2). The Hayward Fault has accumulated energy for over a century. The last large earthquake (M 6.8) occurred in 1868, causing widespread damage throughout East Bay. The earthquake's magnitude was based on an established case study that informs resilience policy-making in the Bay.[45]

We computed the rupture geometry (see Methods) and found that 10 acute care hospitals with 2167 beds (13% of the Bay's total) are located only 5 km away from the rupture. We then estimated the shaking intensities across the Bay (See Methods). Our predictions show that many hospitals will experience violent shaking at a scale not seen in over a century. On average, we predict 51 hospitals will experience peak ground accelerations above 0.2g (Figure 2). In contrast, the M 6.9 Loma Prieta Earthquake, the largest temblor in the Bay since the devastating M 7.9 San Francisco Earthquake in 1906, only exposed 14 hospitals to these shaking levels (Figure 2). For further comparison, Supplementary Figure 2 shows that the recent 2014 M 6.0 Napa Earthquake only exposed a few hospitals to large shaking levels (e.g., only three out of 76 above 0.2g), while the M 7.9 San Francisco Earthquake exposed most of the portfolio to these shaking levels (e.g., 72 out of 76).

We then predicted structural and non-structural damage on the entire portfolio of 426 buildings

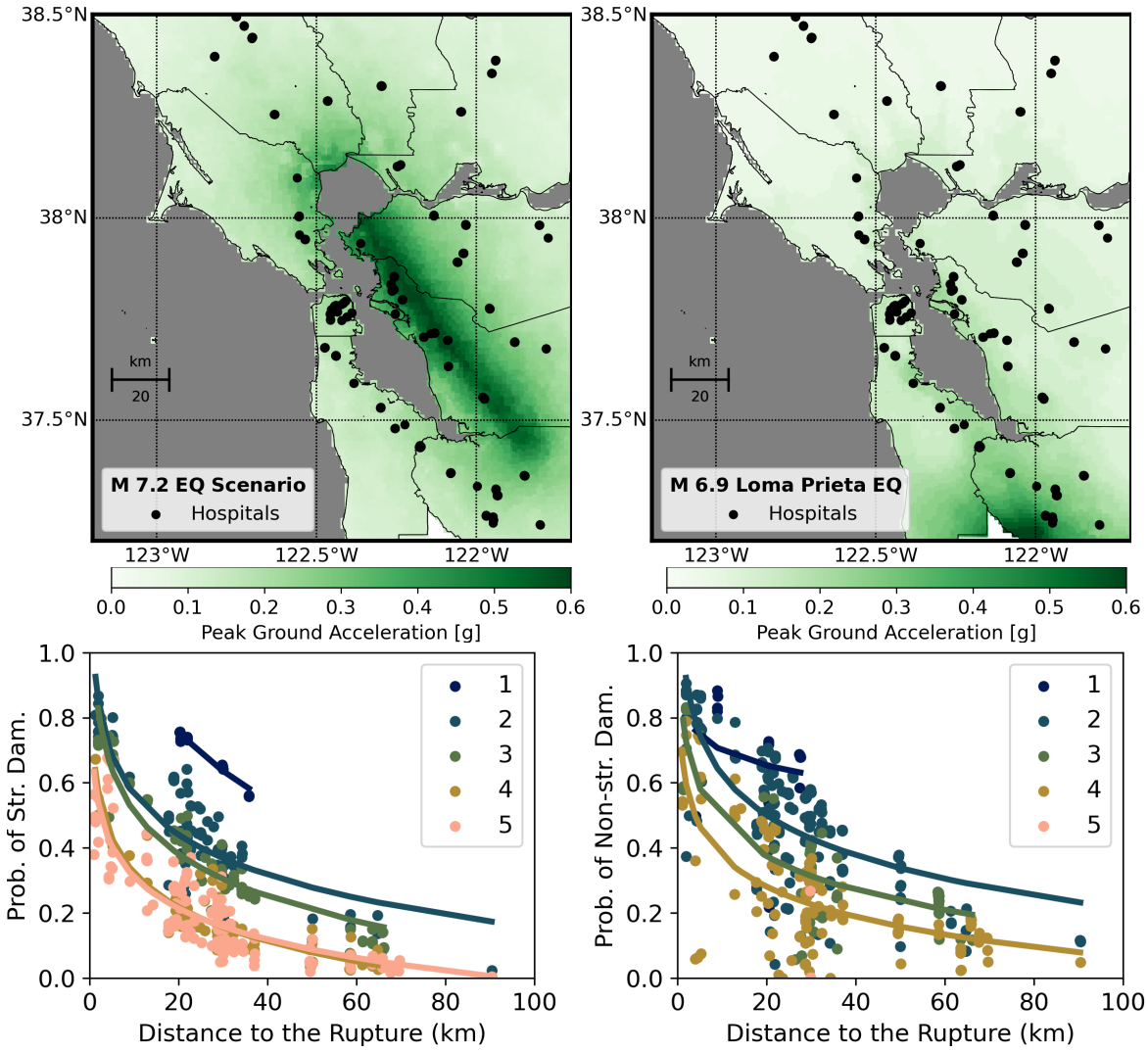

Figure 2: Earthquake disruption simulations. Upper left: Median peak ground accelerations (PGA) due to the M 7.2 earthquake scenario. Upper right: PGAs due to the largest earthquake in more than a century in the Bay. Lower left: Estimated damage probabilities on buildings' structural components for different SPCs (1 to 5). Lower right: Estimated probabilities of damage on buildings' non-structural components for different NPCs (1 to 5)

belonging to the acute care hospitals because both are critical to the continuous operations of healthcare services. We use different damage thresholds as tipping points for service disruption, capturing disruptions at various early stages of damage (see Methods). Hereafter, we denominate the probability of exceeding the threshold "probability of damage" or "probability of failure" of structural and non-structural components for simplicity. Our results show that more than 212 (50% of the total) and 287 (67% of the total) buildings will have probabilities of damage above 0.25 for structural and non-structural components, respectively.

Many hospitals are close to the Hayward Fault and have high infrastructure vulnerabilities (Figure 2). From the 212 buildings with 0.25 or higher probability of structural damage, 152 (72%)

buildings are either 20 km or less from the rupture or have an SPC of 1 or 2. Of the 287 buildings with 0.25 or higher probability of structural damage, 256 (89%) buildings are either 20 km or less from the rupture or have an NPC of 1, 2, or 3. Supplementary Figure 3 compares building fragilities for different structural and non-structural vulnerabilities for reinforced concrete wall buildings, highlighting how this earthquake's shaking can easily damage buildings, especially for low SPC and NPCs.

Post-earthquake Hospital Capacity

Our risk analysis model predicts 8,501 beds will be lost throughout the Bay (see Methods). This means that only 49% of beds will be functional (with a standard deviation of 17%). These losses are significant and highly heterogeneous across the Bay. Figure 3 and Table 1 show our results at the hospital, county, and regional scales. These predictions are based on a threshold of slight damage, i.e., a hospital loses functionality if its structural or non-structural components exceed this threshold (see Methods). Previous earthquakes have shown hospital buildings often lose functionality at these early stages of damage.[21,28–31] Figure 3 and Supplementary Table 3 show the sensitivity of the predictions to the higher damage thresholds, i.e., if doctors decide to keep healthcare operations in buildings exceeding moderate and extensive damage. Across the Bay, the functionality would decrease to 77% and 92% in these cases, respectively, highlighting that building functionality is strongly connected with the damage threshold. However, evidence shows that hospitals are disrupted at earlier stages of damage;[21,28–31] thus, we used slight damage as the threshold for this study.

Table 1: Predicted post-earthquake capacity of functional beds for different Bay counties for a threshold of slight damage. Supplementary Table 3 shows similar results for a threshold of moderate and extensive damage. The numbers in parentheses indicate the percentage in proportion to the pre-earthquake capacity

County	Pre-earthquake	Post-earthquake	
		Mean	Std. Dev.
Alameda	3,221	612 (19%)	513 (16%)
Contra Costa	1,749	812 (46%)	423 (24%)
Marin	627	239 (38%)	188 (30%)
Napa	351	238 (68%)	85 (24%)
San Francisco	3,618	2,245 (62%)	862 (24%)
San Mateo	1,444	886 (61%)	862 (24%)
Santa Clara	4,323	2,200 (51%)	919 (21%)
Solano	722	481 (67%)	168 (23%)
Sonoma	584	424 (73%)	108 (18%)
Total	16,639	8,138 (49%)	2,818 (17%)

We predict the earthquake will significantly impact Alameda County because the Hayward Fault is close to its many communities and vulnerable hospitals (Table 1). Their functional beds decrease to 19% of the pre-earthquake levels (from 3,221 to 612) with a standard deviation of 16%. With 1.6 million people, Alameda is the second largest populated county in the Bay. Thus, the decrease in healthcare capacity will impact many communities. The second most affected county is

Marin, located in the Northern area surrounding the earthquake rupture. Marin's bed capacity will decrease to 38%, but with 251k people, their population is significantly smaller than Alameda's. Thus, Alameda's healthcare system will be the most affected by far.

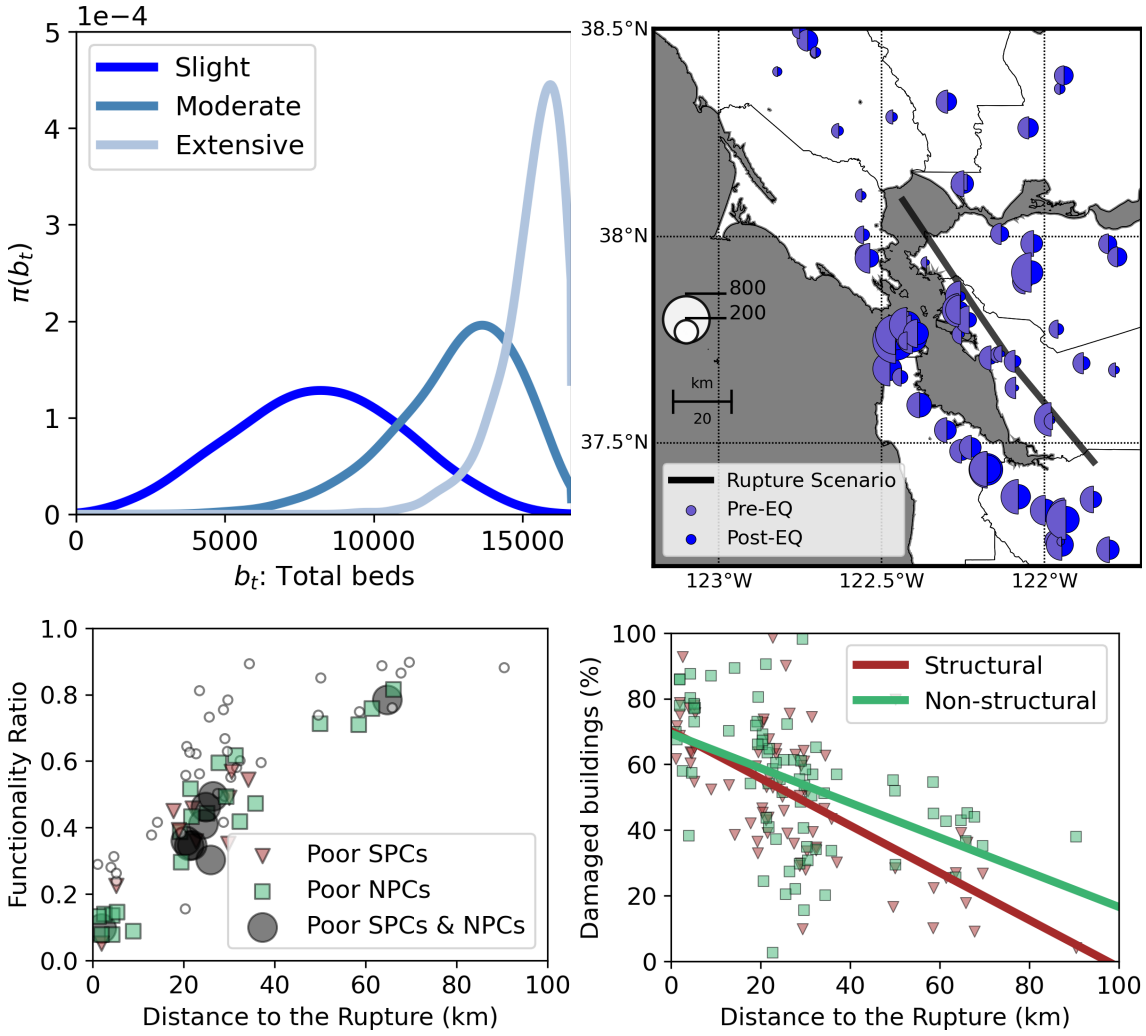

Figure 3: Post-earthquake functionality of the acute care hospital network. Upper left: Probability distribution of functional beds in acute care aggregated in the Bay for three thresholds of disruption: slight, moderate, and extensive. Upper right: Spatial distribution of beds (pre and post-earthquake) across the Bay for the slight damage threshold. Lower left: Expected functionality ratio for each hospital for the slight damage threshold, indicating those hospitals with the top share of low SPCs (i.e., one and two) and NPCs (i.e., one, two, and three). Lower right: (De-aggregated) percentages of buildings with structural and non-structural damage given that the hospital has high functionality loss (i.e., more than 50%).

Figure 3 shows the functionality ratio, i.e., the ratio between the expected number of functional beds after the earthquake and the pre-earthquake conditions (see Methods), as a function of the distance to the rupture. Hospital functionality is significantly lower within 20 km from the rupture, making counties like Alameda particularly at high risk. The average functionality ratio is 24%, 53%, and 83% for hospitals within 20km, between 20 and 40 km, and beyond 40 km, respectively. Figure

3 highlights the hospitals with a high share of buildings with poor SPCs and NPCs to underline that those physical vulnerabilities cascade to significant reductions in hospital capacity. For example, hospitals with the top share of poor SPCs have a 25% smaller functionality ratio than the others, i.e., 39% versus 52%. Hospitals with the top share of NPC buildings have a 30% smaller functionality ratio than the others, i.e., 44% versus 63%.

Figure 3 also points to the relative contribution of structural and non-structural components to hospital disruptions. We analyzed all simulations that led to hospital functionality ratios below 50% to evaluate the percentage of buildings with structural and non-structural damage (see Methods). Figure 3 shows that the contributions vary per the distance to the rupture. Within the first 20 km, hospitals with large disruptions have, on average, 62% and 73% of their buildings with structural and non-structural damage, respectively. At larger distances, however, the relative contributions of non-structural damage increase. For example, beyond 40 km, hospitals with large disruptions have, on average, 26% and 42% of their buildings with structural and non-structural damage, respectively. While the relative contributions from the structural components were slightly smaller than non-structural components, with a ratio of 0.84 (62% versus 73%) within the first 20 km, the ratio of 0.36 (26% versus 42%) beyond 40 km indicates that non-structural components can be a main cause of large hospital disruptions even is the building's structure remains undamaged. Earthquakes can damage non-structural components over large geographical extents because the buildings' dynamics can amplify peak floor accelerations, even at long distances.

Acute Care Accessibility

We predict that the earthquake scenario will radically change healthcare access in the Bay. We coupled the risk model with a network model to assess the cascading effects of earthquakes on healthcare access across the Bay (see Methods). Patients must travel to the next closest hospital if hospitals cannot provide healthcare services, such as those that lose all beds. We also assumed that partially operating hospitals can still provide some healthcare services. We focused on modeling network effects on the hospital and transportation infrastructure for healthcare access.

First, we evaluate network effects on hospitals through travel times and capacity-demand ratios. Our predictions show that the average travel times to the closest acute care hospitals across the Bay increase from 5.9 to 7.4 minutes. This equals a 27% increase with a standard deviation of 97% of the average travel times in pre-earthquake conditions. However, as in the hospital bed capacity, variations of travel times are strikingly different across counties. Patients from Alameda will increase their travel times by 88% (from 4.8 to 9 minutes) due to the significant decrease in their healthcare capacity (Table 2). Marin and Contra Costa patients will increase their travel times by 31% As stated earlier, Alameda and Contra Costa are the second and third most populated counties in the Bay, with 1.7 M and 1.2 M people. Thus, these results highlight that healthcare access will radically change for many.

We found that neighborhoods are even more disproportionately impacted by the earthquake at micro-urban scales. At zip code levels, we observe larger variations in travel time (Figure 4). Communities in the worst zip code increase their travel times by almost five times (from 2.1 to 10.1 minutes), and the eighth zip code is still heavily impacted by the earthquake as its travel time increases by a considerable factor of 4.2 (from 4.2 to 11.6 minutes). Three zip codes in the top eight list have populations of 82, 71, and 35k people. The one with 35k people is in Richmond (Contra Costa County), whereas the ones with 82k and 71k are in Fremont (Alameda County), demonstrating that the earthquake will reshape access to acute care throughout the entire East Bay

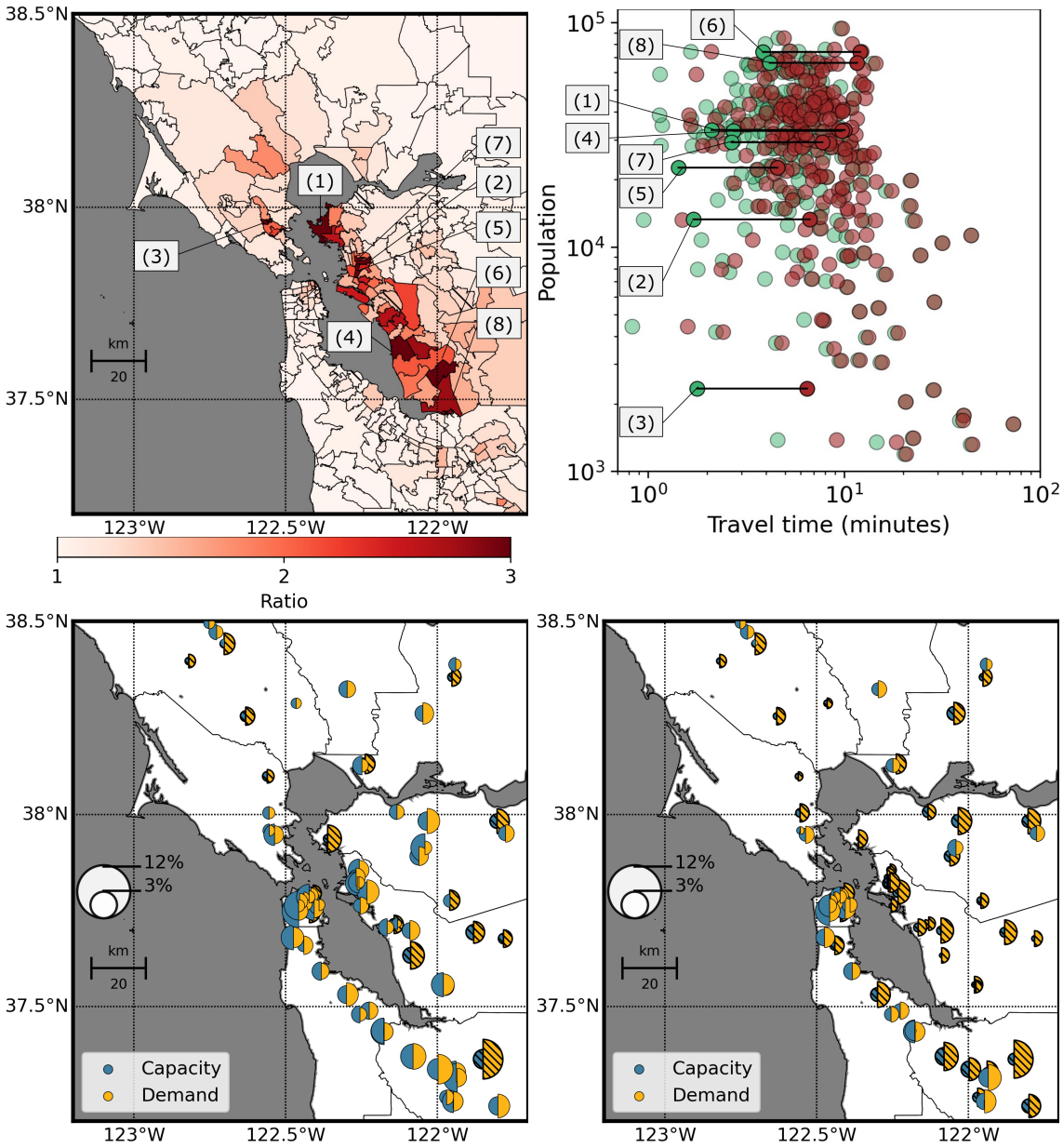

Figure 4: Access to functional acute care hospitals in the Bay Area. Upper left: Rations of post- and pre-earthquake travel times to closest acute care hospitals. Upper right: Variations in travel time at the zip code level and their populations, highlighting the communities most impacted. Lower left: The Ratio between relative demands and capacities before the earthquakes. The ratio between relative demands and capacities after the earthquakes. The ratios above two are highlighted in dashed circles. Notice that the relative capacity is calculated by normalizing the number of beds to pre-earthquake conditions in both cases

from the South part to the North along the earthquake rupture. The neighborhood in Richmond exemplifies the mechanisms by which many of these communities significantly worsen their access to healthcare. Richmond is heavily populated with a single local hospital (number 1 in Figure 1). The hospital is only 5.1 km from the rupture. If the local hospital is lost, communities must travel

Table 2: Travel times (in minutes) to reach to the closest functional acute care hospital before and after the earthquake for different Bay Area counties. The post-earthquake travel times' mean and standard deviation values as a percentage of the travel time before the earthquake are included in parentheses.

County	Pre-earthquake	Post-earthquake		Population (thousands)
		Mean	Std. Dev.	
Alameda	4.8	9.0 (188%)	3.8 (79%)	1,682
Contra Costa	7.8	9.6 (122%)	2.0 (26%)	1,166
Marin	7.8	10.2 (131%)	3.4 (43%)	251
Napa	6.9	7.3 (106%)	1.8 (26%)	138
San Francisco	2.8	3.2 (113%)	0.9 (31%)	874
San Mateo	5.3	5.7 (106%)	0.8 (15%)	764
Santa Clara	5.7	6.5 (113%)	1.3 (22%)	1,936
Solano	7.0	7.5 (106%)	1.3 (18%)	453
Sonoma	9.2	9.6 (104%)	0.9 (9%)	489
Total	5.9	7.4 (127%)	5.7 (97%)	7,753

south outside Richmond to Berkeley or Oakland. However, if these hospitals also fail, given their proximity to the rupture, Richmond communities will have to travel longer from East to West Bay to reach San Rafael.

To systematically evaluate how failures of hospitals cascade beyond their catchment area, we assessed the ratio between the relative demand and capacity (see Methods). We computed the relative number of functional beds per hospital and divided it by the relative demands for healthcare, i.e., if the ratio is close to one, the hospital capacity will match the relative demands for healthcare in the Bay. We found that many hospitals had high ratios before the earthquake, highlighting disparities in healthcare access and worse conditions in East Bay. Nineteen hospitals (25%) had ratios above two (Figure 4); five are in Alameda, and three are in Contra Costa counties, both in East Bay (Supplementary Table 4). In contrast, in West Bay, San Mateo has no hospital with such ratios. We found that the earthquake exacerbates these disparities. After the earthquake, 44 hospitals will have ratios above two, 2.3 times as many as in pre-earthquake conditions. However, in Alameda, sixteen hospitals go above this threshold, 3.2 times as many as in pre-earthquake conditions. These effects propagate even to regions with fewer hospital disruptions since they also have to absorb patients from other catchment areas. For example, in Santa Mateo County in West Bay, 33% of their hospitals will have ratios above two after the earthquake, even though no hospital had such ratios before.

Second, we network effects on the transportation infrastructure because it supports healthcare access (see Methods). Figure 4 shows the relative volume of travels with destination to the closest acute care hospitals. Figure 4 also shows the road usage for pre-earthquake conditions. The thickness represents the road usage volume, and in brown, we point to the roads with usage above the 90th percentile to highlight those most important. Before the earthquake, unsurprisingly, we observed that the most important roads were close to the hospitals. The road importance increases for those areas that are highly populated (e.g., the two hospitals in Fremont serving the communities including those in zip code with 4th, 6th, and 8th largest increases in travel time) and that have

fewer hospitals (e.g., the two hospitals in Richmond serving the communities including the zip code with the largest increases in travel time).

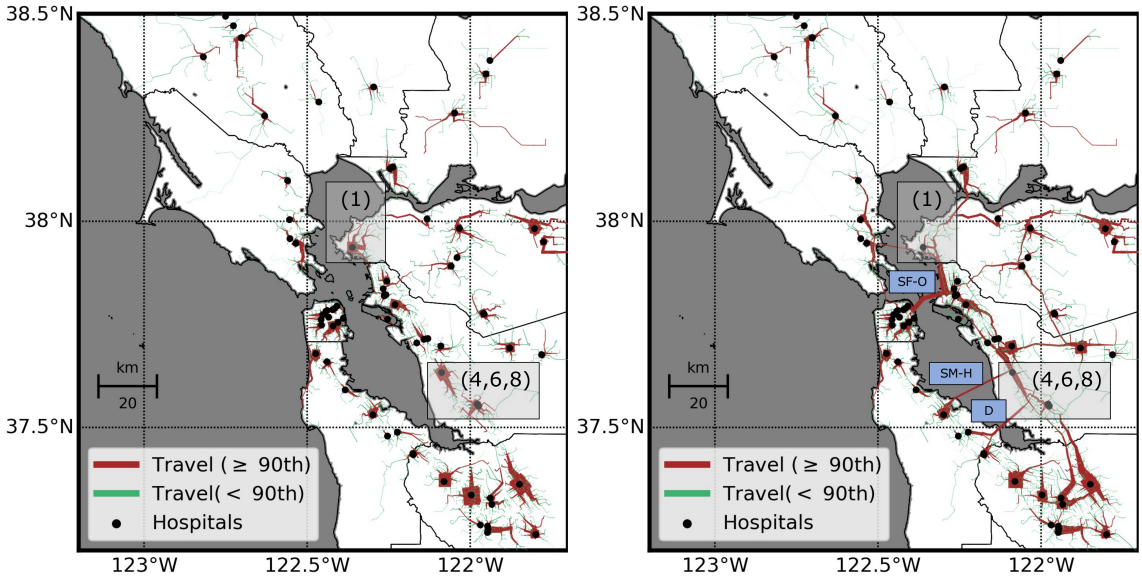

Figure 5: Mobility to reach the closest functional acute care hospital in the San Francisco Bay. left: Travel volumes to reach the closest acute care hospital before the earthquake, indicating the hospitals serving the zip codes with the 1st, 4th, 6th, and 8th top rations of travel time variations. Right: Projections of travel volumes to reach the closest acute care hospital after the earthquake.

Figure 4 also shows the volumes of travel after the earthquake, highlighting in brown the roads above the threshold defined in pre-disaster conditions. We observe that patient mobilizations will undergo significant changes after the earthquake. Many roads will experience large volumes over longer distances than pre-earthquake conditions. For example, Figure 4 clearly shows how people in the Richmond communities must travel longer as the brown lines connect with the local hospital with significantly lower intensity, and instead, the ones that connect them to hospitals in neighboring become thicker and longer. More strikingly, Figure 4 clearly shows that these effects are heavily pronounced for many communities in East Bay that will have to travel to the West Bay in search of acute care hospital services. Three main bridges connect East with West Bay through the Oakland-San Francisco Bay Bridge, the San Mateo-Hayward Bridge, and the Dumbarton Bridge. Figure 4c shows that no patient has to cross these bridges to reach their closest acute care hospitals. However, if hospitals in East Bay fail, the travel volume in these bridges becomes highly important, reaching values 7.8, 3.2, and 4.2 times higher than the roads with the largest volumes of travel (90th percentile) if no hospitals fail.

Discussion

We present a modeling framework to investigate the post-earthquake access to acute care hospitals. The framework combines probabilistic risk analysis with network modeling to investigate disruptions of healthcare services across multiple Bay Area communities. Using novel data, we rigorously study the entire Bay Area's acute care portfolio with 76 hospitals (and 426 buildings), considering their

infrastructure risks, healthcare capacity, and interdependencies, coupled with the transportation system (see Methods).

First, we find that services within hospital buildings will be highly disrupted. We predict that, in total, 51% of beds will be lost due to building damage, reducing the acute care capacity from 16,639 to 8,138 beds. In Alameda County, we predict the effects to be more pronounced, with only 19% of functional beds, reducing its capacity from 3,221 to 612 beds. These results strongly highlight the need for substantial preparedness to face future earthquakes in the Bay Area. We modeled physical failures within buildings to study potential scenarios where the buildings' components will not be non-operational. Encouragingly, previous earthquakes have shown that medical personnel can adapt to emergencies by reconfiguring spaces that remain functional (or safe) after earthquakes. For example, the large Christchurch Hospital moved its triage area to the parking lot after the 2011 New Zealand Earthquake.[46] Similarly, the Mustafa Kemal University Hospital's personnel in Turkey moved their surgery activities from the upper floors to the first story initially. Later, the personnel moved their entire emergency department to the parking lot.[35] If hospitals in the most affected areas (e.g., Alameda County) prepare in advance to use different exterior spaces or interior spaces that remain safe, e.g., by ensuring that there is enough space or that water and power can still work for the exterior parts of the building, these hospitals may be able to recover, at least, some partial functionality, instead of altogether dropping most of their capacity. In an emergency, quickly recovering capacity is essential. Many patients may require immediate treatment, especially those from neighborhoods close to the earthquake source, since they may be most affected.

Second, our results suggest that structural and non-structural building components must be retrofitted to improve post-earthquake healthcare access. While retrofits have typically focused on the main structure, past earthquakes show us that non-structural component failures frequently cause loss of hospital functionality after earthquakes. For example, the Christchurch Hospital had no structural damage after the 2011 Earthquake. However, damaged backup generators disrupted intensive care units, the radiology department, and emergency services.[28,46] Similarly, researchers surveyed affected hospitals after the 2016 Kumamoto Earthquake. They found that 80% of the facilities had water connection failures (but minimal or no structural damage) that disrupted critical services such as hemodialysis and sterilizations.[30,31] In California, hospitals with SPCs of 2 or lower and NPCs of 3 or lower are mandated to be retrofitted by 2030. Meeting this deadline would be a tremendous achievement for the resilience of hospitals. However, hospitals are unlikely to meet this resilience goal as they have already manifested that they are under financial stress and that the investments to achieve this goal are massive, as 24% and 69% of buildings have SPCs of 2 or below and NPCs of 3 and below.[19] If the goal is unachievable by 2030, Bay Area hospitals can still enhance the system's resilience by investing strategically in retrofitting those hospitals that serve larger catchment communities. In addition, retrofit costs are often higher for structural components than non-structural components since a structural retrofit often requires adding strength, (often) stiffness, and ductility to the core structural system. In contrast, non-structural components can often be strengthened by adding anchors to different equipment and elements without significant interventions to the building's backbone. Our results show that non-structural component failures frequently cause functionality loss, especially at large distances from the ruptures. Thus, targeting non-structural components, especially for those buildings that are already structurally sound (e.g., SPCs of 3 and higher), seems to be an effective way to enhance post-earthquake access to healthcare over large regions.

Third, our results suggest significant and highly heterogeneous changes in hospital access after

the earthquake, with substantial implications in the short and long term. The average travel time to the closest hospital increases by 27%, from 5.9 to 7.4 seconds. We predict that Alameda County will be affected the most, with an overall increase of 88%, but with zip codes that can experience even four or five times longer travel times than pre-earthquake conditions. These longer travel times will redefine the access to acute care services and medical equipment needed to treat critically injured patients after an earthquake. For example, people with severe exposed fractures, a common trauma injury in buildings that collapse, will require x-ray machines and surgery that can be found in acute care hospitals. Similarly, acute care hospitals often have dialysis machines that can be vital to treating patients with kidney failures from crush syndrome, a condition that develops if trapped people in collapsed buildings have crushing injuries to skeletal muscle for a long time before being rescued. Thus, our results suggest that Alameda communities will travel disproportionally longer to access these critical services, which can have lethal consequences for many people because the earthquake scenario in the Hayward Fault is also likely to cause high-severity injuries there. To mitigate these disproportionate impacts, the Bay Area needs to elaborate emergency response plans to rapidly deploy temporary healthcare facilities that help alleviate the deficit for healthcare in an emergency in the East Bay. In addition, the Bay Area's plans need to consider long-term public health. Hospitals require a long time to be repaired, especially if both structural and non-structural components are compromised; thus, disruptions can affect communities for years. Non-earthquake emergencies, e.g., from accidents or sudden illnesses like cardiac arrests, require rapid delivery of healthcare treatment. Thus, even in the long term, Alameda communities will face disproportionate access to healthcare. Reconstructing and repairing the hospital infrastructure strategically and promptly will be fundamental to protecting many communities.

Fourth, our results highlight the strong coupling between the transportation and the hospital networks. We modeled disruptions to different hospitals and demonstrated the differential importance of roads for healthcare access before and after the earthquake. We show that roads leading to hospitals become more crowded over long distances. Such large volumes will require traffic plans, especially in a post-earthquake scenario, when many people must reach emergency treatment simultaneously. Our analysis did not include failures in the transportation system to study the impact of hospital vulnerabilities on healthcare access cleanly. However, recent studies on the vulnerability of the transportation system indicate that earthquakes can also make several bridges fail in the Bay Area, further exacerbating healthcare access. Studies indicate that many communities in Alameda County are at risk of experiencing delays in traveling time by car as many bridges could collapse.[47] As the Bay Area relies heavily on car traffic, these studies and our findings suggest that healthcare access could be greatly impacted by an earthquake. We found that many communities in East Bay will have to travel to the West Bay to access acute care hospitals using the Bay Bridge, San Mateo-Hayward Bridge, or the Dumbarton Bridge. Studies indicate that smaller bridges serving as access points to these three critical bridges are either at moderate or high collapse risks due to earthquakes.[47] The San Mateo-Hayward Bridge has even been pointed out to be at high risk. Thus, many communities may be unable to cross the West Bay after an earthquake. Thus, planning for an earthquake emergency in the Bay Area requires considering the vulnerabilities of multiple infrastructure systems. Retrofitting bridges will have an important effect in mitigating the impacts of earthquakes on healthcare access, but for that, the retrofit program needs to consider the relative importance of different bridges across the city.

Methods

Risk Formulation: For single to multiple buildings

We utilize an extension of the performance-based earthquake engineering (PBEE) framework, initially established to assess earthquake consequences in an infrastructure unit, and analyze multiple hospital buildings.[48–50] Under Markovian (conditional independency) assumptions described in canonical PBEE formulations,[49,50] we find the probability distribution of an earthquake consequence, e.g., economic losses or fatalities, as

$$P_{DV,DS,IM}(dv, ds, im) = P_{DV|DS}(dv|ds)P_{DS|IM}(ds|im)P_{IM}(I'm), \tag{1}$$

where $P()$ is a probability distribution (or mass) function, and DV is a random variable representing an earthquake consequence (also called a decision variable). For example, DV can track repair costs in buildings. In this case, DV will be a positive number with an upper bound of dv_u, i.e., the total replacement cost of the building. In other applications, DV has a different variable space, e.g., $DV \in \mathbb{Z}$ for the number of injured people in a building.[3,4] DS is an ordinal random variable that evaluates structural damage in an infrastructure unit, and typically $DS \in \{$None, Slight, Moderate, Extensive, Complete$\}$. Finally, IM is a random variable representing an intensity measure of shaking at the building site, and generally, $IM \in \mathbb{R}_{\geq 0}$. Note that earthquake shaking on the Earth's crust has a physical upper bound, but such a bound is not generally modeled since extremely high shaking cannot produce a bigger DS than Complete, thus barely impacting seismic risk analysis. Frequently, DS and IM are marginalized from $P_{DV,DS,IM}(dv, ds, im)$ (e.g., through summation and integration) to find $P_{DV}(dv)$.[48–50]

Lee and Kiredmjian[51] first formalized the extension of the PBEE formulation to multiple infrastructure units,[52–54,54,55] focusing on transportation infrastructure. After finding marginal distributions of damage in single units, they formulate joint distributions of damage for all units by defining spatial correlations and their decay for distant sites. However, in the last two decades, empirical studies have better characterized spatial correlation on shaking (i.e., IM) rather than building damage.[56–59] To account for it, Ceferino et al.[3] first formulated an extension of regional PBEE incorporating earthquake shaking's spatial correlation, defining fully the set of conditional independencies in state-of-the-art regional risk models and applications.[60–63] Ceferino et al.[3] defined the regional model for earthquake casualties, and here we apply it to hospital functionality in a region.

We redefine the traditional PBEE notation to keep the equations concise in the extension to a regional analysis with many buildings. We denote a random variable X's probability distribution $P_X(x) = \pi(x)$. Similarly, for a multi-variate vector $\boldsymbol{X}$, we denote its probability distribution $P_{\boldsymbol{X}}(\boldsymbol{x}) = \pi(\boldsymbol{x})$, where $\boldsymbol{x}$ is a specific realization of $\boldsymbol{X}$. Using this notation, we define the damage ordinal variable D, instead of DS, and call D_k^s and D_k^n the structural and non-structural damage of building k. Thus, we are interested in the damage vector $\boldsymbol{D} = \{D_1^s, D_1^n, \ldots, D_m^s, D_m^n\}$, where m is the total number of buildings in the region. We also define the shaking variable I, instead of IM, and call I_k^s and I_k^n the shaking measure affecting structural and non-structural damage of building k. For example, I_k^s can be the peak ground acceleration or spectral acceleration affecting the structural components, and I_k^n is the peak floor acceleration affecting acceleration-sensitive non-structural components, e.g., ceilings. Thus, we are interested in the shaking intensity vector $\boldsymbol{I} = \{I_1^s, I_1^n, \ldots, I_m^s, I_m^n\}$, where m is the total number of buildings in the region. We extend

the Markovian (or conditional independence) assumptions from single buildings[49,50] to multiple buildings[3] to estimate the joint probability distribution of damage and intensity vectors as

$$\pi(\boldsymbol{d}, \boldsymbol{i}) = \pi(\boldsymbol{d}|\boldsymbol{i})\pi(\boldsymbol{i}) \tag{2a}$$

$$\pi(\boldsymbol{d}|\boldsymbol{i}) = \prod_{k=1}^{m} \pi(d_k^s|i_k^s)\pi(d_k^n|i_k^n), \tag{2b}$$

where $\boldsymbol{d} = \{d_1^s, d_1^n, \ldots, d_m^s, d_m^n\}$ and $\boldsymbol{i} = \{i_1^s, i_1^n, \ldots, i_m^s, i_m^n\}$ are specific realizations of $\boldsymbol{D}$ and $\boldsymbol{I}$, respectively. Eq. 2b assumes damage is independent at different buildings conditioned on their respective shaking intensities; thus $\pi(\boldsymbol{d}|\boldsymbol{i})$ can be estimated as the product of probability distributions of damage in each building. However, unconditional damages will be correlated through the joint probability distribution of shaking in the region, $\pi(\boldsymbol{i})$. Similarly, we assume that structural and non-structural damage (D_k^s and D_k^n) within a building k are conditionally independent given their respective shaking intensities (I_k^s and I_k^n). Yet, these two random variables of damage will be correlated since these shaking intensities in the building are also correlated, e.g., peak ground acceleration and peak floor acceleration. Figure 6 illustrates and summarizes all conditional dependencies through a probabilistic graphical model.

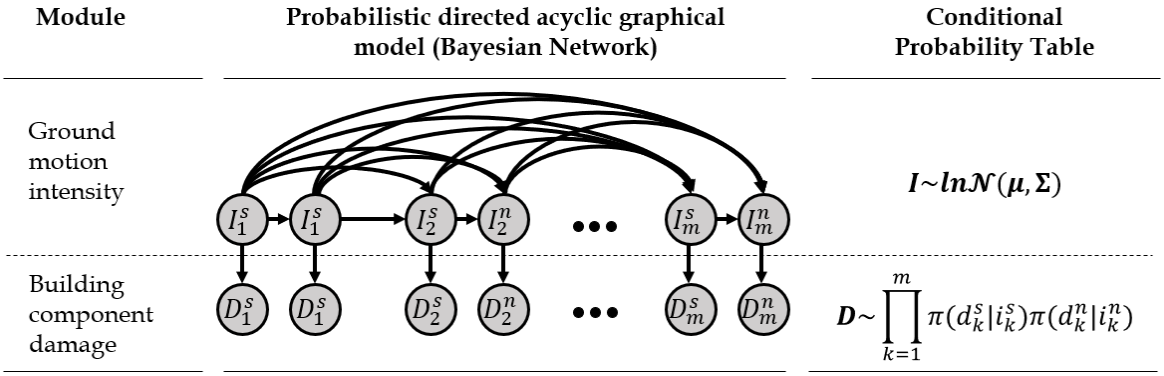

Figure 6: Probabilistic graphical model (Bayesian network) representing the joint distribution of the risk model to assess structural and non-structural damage from earthquake ground motion intensities.

We assess the building functionality vector $\boldsymbol{F} = \{F_1, \ldots, F_m\}$, where F_m is a Bernoulli random variable that assesses whether the hospital building k will work ($F_k = 1$) after the earthquake. We model F_k as a deterministic function of the structural and non-structural damage of the building as an input. Thus, under a change of variables, Eq. 2 becomes

$$\pi(\boldsymbol{f}, \boldsymbol{i}) = \pi(\boldsymbol{f}|\boldsymbol{i})\pi(\boldsymbol{i}) \tag{3}$$

where $\boldsymbol{f} = \{f_1, \ldots, f_m\}$ is a specific realization of $\boldsymbol{F}$. Figure 7 illustrates and summarizes all conditional dependencies through a probabilistic graphical model. Note that a probabilistic formulation that links damage to functionality could also be incorporated, introducing an additional term to Eq. 3, similar to Eq. 1. Thus, our approach admits such extensions.

Hospitals can rapidly lose functionality at early stages of structural and non-structural damage, as observed in the 2023 M 7.8 Kahramanmaras Earthquake in Turkey,[10] 2011 M 6.1 Christchurch

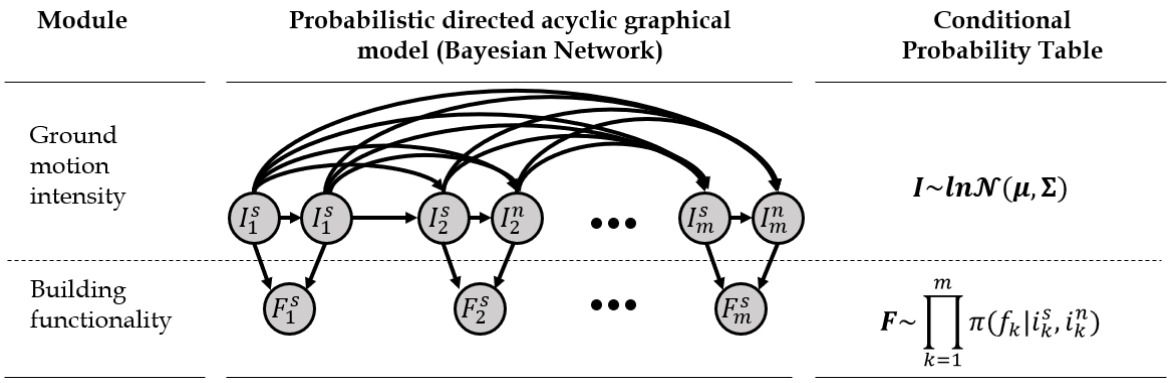

Figure 7: Probabilistic Graphical Model representing the joint distribution of the risk model to assess hospital functionality from earthquake ground motion intensities.

Earthquake in New Zealand,[21] and 2010 M 8.8 Maule Earthquake in Chile.[64] We consider that damage thresholds, d^s and d^n, for the structural and non-structural components trigger the disruption of hospital functionality, i.e., if either fails, the hospital loses functionality. We can estimate the probabilities of not exceeding these thresholds as $p_k^s = \pi(D_k^s \leq d^s | I_k^s = i_k^s)$ and $p_k^n = \pi(D_k^n \leq d^n | I_k^n = i_k^n)$, respectively, which can be evaluated with earthquake fragility functions. Thus, we can model functionality as the intersection of both random events, i.e., the structural and non-structural components work after the earthquake. Since D_k^s and D_k^n are conditionally independent, the F_k is a Bernoulli random variable with probability $p_k^s p_k^n$. Accordingly,

$$\pi(\boldsymbol{f}|\boldsymbol{d}) = \prod_{k=1}^{m} \left[p_k^s p_k^n\right]^{f_k} \left[1 - p_k^s p_k^n\right]^{1-f_k} \tag{4}$$

The functionality of the hospital relies on the structural and non-structural components as described in Eq. 4. The hospital portfolio has various levels of SPC and NPC that control the final functionality of the hospital.

We are also interested in the probability distribution of the total number of functional beds B_t in the region, which can be estimated as

$$B_t = \sum_{k=1}^{m} \beta_k F_k \tag{5}$$

where β_k is the number of beds (all functional before the earthquake) at the hospital building k. We are also interested in estimating the distributions of the total number of functional beds B_h in hospital h as each hospital can have multiple buildings with beds. Let $\boldsymbol{k_h}$ be the set containing all indexes of the buildings belonging to the hospital h. Thus,

$$B_h = \sum_{k \in \boldsymbol{k_h}} \beta_k F_k \tag{6}$$

In addition, we want to evaluate the contributions of structural and non-structural damage in buildings to the loss of functionality on the hospital campus. We can model the expected number of buildings with structural damage in a hospital campus given that the hospital only has a portion ϕ of functional beds as

$$\mathbb{E}\Big(\sum_{k\in\boldsymbol{k_h}} 1\{D_k^s > d^s\}\Big| B_h < \phi\sum_{k\in\boldsymbol{k_h}}\beta_k\Big) = \sum_{k\in\boldsymbol{k_h}} \frac{\pi(D_k^s > d^s \cap B_h < \phi\sum_{k\in\boldsymbol{k_h}}\beta_k)}{\pi(B_h < \phi\sum_{k\in\boldsymbol{k_h}}\beta_k)} \tag{7}$$

Similarly, we can evaluate the number of buildings with nonstructural damage in a hospital campus given that the hospital only has a portion ϕ of functional beds as

$$\mathbb{E}\Big(\sum_{k\in\boldsymbol{k_h}} 1\{D_k^n > d^n\}\Big| B_h < \phi\sum_{k\in\boldsymbol{k_h}}\beta_k\Big) = \sum_{k\in\boldsymbol{k_h}} \frac{\pi(D_k^n > d^n \cap B_h < \phi\sum_{k\in\boldsymbol{k_h}}\beta_k)}{\pi(B_h < \phi\sum_{k\in\boldsymbol{k_h}}\beta_k)} \tag{8}$$

Approaches for numerical solutions

Regional seismic risk analysis is a hyper-dimensional problem. $\pi(\boldsymbol{f},\boldsymbol{i})$ in Eq. 3 can be analytically evaluated because $\pi(\boldsymbol{f}|\boldsymbol{i})$ and $\pi(\boldsymbol{i})$ have closed-form expressions.[57–59,65] However, $\pi(\boldsymbol{f})$ cannot be analytically evaluated because it requires the marginalization of correlated random variables, i.e., in $\boldsymbol{i}$, which involves integration without closed-form solutions. Conducting marginalization operations through numerical integration (e.g., Reimann integration) also becomes computationally intractable, even for a few buildings.[3] Thus, modern seismic risk analysis models are often solved using Monte Carlo to find regional earthquake consequences, such as $\pi(\boldsymbol{f})$.

Risk modelers also compute the distribution of aggregated earthquake consequences, such as total repair costs in regions. In our analysis, we seek to estimate the probability distribution $\pi(b_t)$, the sum of functional beds from different hospital buildings. $\pi(b_t)$ cannot be solved analytically, and numerical integration is computationally intractable even for a few buildings.[3] Thus, we often solve these high-dimensional problems with Monte Carlo. Other techniques can also find $\pi(b_t)$ with high computational efficiency when the number of buildings is large enough through approximations of $\pi(b_t|\boldsymbol{i})$. Ceferino et al.[3,4] utilized techniques arising from the Central Limit Theorem (CLT) to show both theoretically and empirically when and why these approximations can be accurate and computationally efficient. Later, Heresi and Miranda[55] empirically showed that similar approximations work under mild correlation conditions in seismic risk models.

Since hospitals have different numbers of buildings, from a few to many, this study uses Monte Carlo to solve our risk model instead of the approximations from CLT. We leveraged the Natural Hazards Engineering Research Infrastructure (NHERI) SimCenter's R2D tool[66–68] to set up and compute $\pi(\boldsymbol{i})$ and $\pi(\boldsymbol{d},\boldsymbol{i})$ in Eq. 2. We used R2D to generate 5,000 realizations of $\boldsymbol{i}$ and $\boldsymbol{d}$. We used them to compute $\boldsymbol{f}$, B_h for each hospital, and B_t in the entire region.

Earthquake Rupture and Shaking Modeling

We study an M 7.25 earthquake scenario on the Hayward Fault. Similar scenarios have been extensively studied to inform resilience policy-making in the Bay Area.[45] The rupture geometry was obtained from the Uniform California Earthquake Rupture Forecast (UCERF) 2.[69] The earthquake ruptures the Hayward South and North sections over a total length of ∼110 km.

Estimates of shallow shear wave velocities (averages at the top 30 m of soil) are utilized over the entire Bay Area.[70] With this information, we built the joint probability distribution of shaking intensities $\pi(\boldsymbol{i})$ in R2D. We utilized a state-of-the-art ground motion model[71] for shallow crustal earthquakes to estimate medians and logarithm standard deviations of $\boldsymbol{i}$. $\boldsymbol{i}$'s uncertainty is divided into two components.[72] The first component captures between-event uncertainty and affects the

entire region equally, but it varies per intensity measure type, e.g., peak ground acceleration versus spectral acceleration. The first component captures correlation across different intensity measures.[73] The second component captures within-event uncertainty and affects the entire region and intensity measure types differently. This component captures spatial correlation and correlation across different intensity measure types. We use a computationally efficient method to account for the second component.[59,74] As stated earlier, we sampled 5,000 realizations of $\boldsymbol{i}$ and show expected values $\mathbb{E}(\boldsymbol{i})$ for the entire region (Figure 1). Notice that for illustration purposes, we show $\mathbb{E}(\boldsymbol{i})$ for the entire Bay Area ($+10,000$ locations), but for the hospital network's risk analysis, we only need to quantify $\boldsymbol{i}$ at the 426 building locations.

Vulnerability modeling

This paper utilized building-level lognormal fragility functions to determine damage to structural and non-structural components. For example, to determine the likelihood of not exceeding a structural damage threshold d^s in building k as a function of the shaking intensity measure, we use fragility functions like

$$\pi(D_k^s \leq d^s | I_k^s = i_k^s) = \Phi\left(\frac{log(i_k^s) - log(\alpha)}{\beta}\right) \tag{9}$$

where Φ is the standard normal cumulative distribution function.[75] The parameters α and β define the fragility function and vary according to the damage threshold d^s and the building's structural type and vulnerability (e.g., SPC rating) for building k. α equals the shaking intensity (e.g., PGA) that exposes the building to a 50% probability of damage of at least d^s. β is a normalizing factor that defines the width of the transition range between shaking with low and high damage probability, and it is a measure of aleatory uncertainty in the vulnerability analysis. In the limit, when $\beta \to 0$, Eq. 9 becomes equivalent to a deterministic assessment, where the building would fail after a fixed shaking threshold. An analogous equation is used for non-structural damage.

We assess structural damage for the variety of structural systems types and five levels of structural vulnerability (Figure 1 and Supplementary Figure 1). We used and adapted structural fragility functions developed in HAZUS,[76] also available in R2D,[77] to obtain this wide variety of fragility functions. Following the definitions of SPC ratings (Supplementary Table 1), we mapped SPC 1, and 2 to pre-code and moderate-code fragility functions for regular buildings from HAZUS,[76] i.e., we used those α and β values for Eq. 9. Note that SPC 1 and 2 category does not comply with the structural provisions of the Alquist Act. In contrast, SPC 3, 4, and 5 comply with the Alquist Act. Fragility functions for SPC 5 buildings are obtained by increasing all the α values for high-code structures by 50% higher PGAs. These adjustments were made to represent that hospitals designed to meet the Alquist Act (SPC 5) according to the ASCE7-16 building code are designed to withstand 50% higher seismic loads than regular buildings, i.e., an importance factor of 1.5.[78] SPC 3 buildings are steel structures that comply with the Alquist Act but are pre-Northridge. We used regular building fragility functions to represent the vulnerability of SPC buildings as pre-Northridge's non-ductile connections as it takes $\sim$30% less seismic demands to make them reach moderate and extensive levels of damage,[79] i.e., $0.7 \times 1.5\alpha =\sim \alpha$. Finally, we modeled SPC 4 buildings with 1.25α to represent that these buildings have lower performance than SPC 5 buildings (1.5α). SPC 4 buildings comply with the Alquist Act but can have some structural

conditions that make them more prone to damage, e.g., lack of weak beam/strong column, presence of short captive columns.[80]

We followed a similar approach for the fragility functions of buildings' non-structural components (Supplementary Table 2). We mapped NPC 1, 2, and 3 to pre-code, moderate-code, and high-code fragility functions for acceleration-sensitive non-structural components from HAZUS.[81] For NPC 4 and 5, we adjusted the fragility functions of high-code fragility functions by increasing the median PFA to reach different damage states by 25% and 50%, respectively. Unlike structural components, we defined the same fragility functions for all building types because hospitals have similar non-structural components, e.g., equipment for acute care. However, as stated earlier, the input PFA for each hospital building differs and depends on the structural type since we use spectral acceleration as a proxy.

After defining these fragility functions for the portfolio of hospital buildings, we computed realizations of building damage utilizing R2D.[82] As mentioned, we generated 5,000 samples of the buildings' structural and non-structural damage for each ground-shaking simulation. Figure 2 shows $\pi(D_k^s > d^s)$ and $\pi(D_k^n > d^n)$, the distribution of damage for the structural and non-structural components. As stated earlier, we initially tested multiple thresholds of damage, d^s and d^n (e.g., slight, moderate, extensive damage) to evaluate hospital disruptions (Figure 3). However, we used the slight damage threshold for most of the analysis later in the study since most hospitals lose functionality at quite early stages of damage.

At each building k, we used the Peak Ground Acceleration (PGA) as the shaking intensity random variable I_k^s to estimate structural damage. While spectral accelerations can also be used to improve damage predictability through the inclusion of structural properties, such as period of vibration,[4] we did not follow this approach here since fragility spectral acceleration-based fragility functions are not available for the diversity of building typologies in the San Francisco Bay.

We used Peak Floor Acceleration (PFA) as the shaking intensity random variable I_k^n to estimate non-structural damage at building k. We focused on PFA because acceleration-sensitive non-structural components (e.g., ceilings and shelves) often fail before drift-sensitive non-structural components. In addition, acceleration-sensitive components, such as x-ray equipment, are often more critical for the functionality of the hospital. PFA varies along the building height, and the total non-structural damage depends on the distribution of non-structural components in the building stories, but such data are often unavailable. Thus, we utilize a proxy for a representative PFA equal to the spectral acceleration at the building's period of vibration. Further studies can enhance the fidelity of this analysis if higher-resolution information for non-structural components is available, e.g., on each floor.

Network Model: Acute care Accessibility Modeling

We denote $G = (\boldsymbol{v}, \boldsymbol{e})$ a graph, where $\boldsymbol{v}$ is the set of $|\boldsymbol{v}|$ vertices and $\boldsymbol{e}$ the set of $|\boldsymbol{e}|$ edges. This graph will represent the infrastructure system of hospitals and roads supporting healthcare access in the Bay Area. Let $p \in \boldsymbol{p}$ be a vertex representing the location of a patient needing acute care and $\boldsymbol{p}$ be the set of all patient vertices. Also, let $h \in \boldsymbol{h}$ be a vertex representing the location of an acute care hospital and $\boldsymbol{h}$ be the set of all hospital nodes. In this case, $\boldsymbol{p} \subseteq \boldsymbol{v}$, and $\boldsymbol{h} \subseteq \boldsymbol{v}$. $\boldsymbol{e} = \{(u, v) | u, v \in \boldsymbol{v}\}$ is the set of $|\boldsymbol{v}|$ edges representing different roads connecting different locations (vertices) in the region. We denote $\tau(u, v) \in \mathbb{R}_{\geq 0}$ the travel time between vertices u and v.

To analyze healthcare access, we evaluate the shortest travel times for a patient in node p to reach any hospital vertex in the set $\boldsymbol{h}$. We modeled hospital h as a source vertex and found the

shortest paths to all vertices $p \in \boldsymbol{p}$ simultaneously, resulting in a shortest-path tree problem. This approach is faster than computing multiple shortest for each pair h and p, separately. Thus, for each vertex h, we find

$$\min_{(u,v) \in \boldsymbol{e}} \sum \tau(u,v)x(u,v) \tag{10a}$$

$$\text{s.t.} \quad \sum_{v:(u,v)\in \boldsymbol{e}} x(u,v) - \sum_{v:(v,u)\in \boldsymbol{e}} x(v,u) = b_u, \quad \forall u \in \boldsymbol{v} \tag{10b}$$

$$b_u = |\boldsymbol{p}| \quad \text{for} \quad u = h \tag{10c}$$

$$b_p = -1 \quad \text{for} \quad u \in \boldsymbol{p} \tag{10d}$$

$$b_u = 0 \quad \text{for} \quad u \neq h, p \tag{10e}$$

$$x(u,v) \in \{0,1\}, \forall (v,u) \in \boldsymbol{e} \tag{10f}$$

This optimization problem seeks to find the minimum travel time from vertex h to all vertices in $\boldsymbol{p}$ simultaneously. This optimization problem can also be interpreted as a special network flow problem where we seek to find a directed path with minimum cost from a source node h to multiple destinations. $\tau(u,v)$ can be interpreted as edge flow cost, and the shortest path problem can be seen as sending a flow unit to each destination in $\boldsymbol{p}$. We solve Eq. 10 to find the shortest travel time $t^*(p,h)$ from each node in $\boldsymbol{p}$ to each (hospital) vertex h (Figure 8). We can use multiple algorithms to solve Eq. 10, including Dijkstra and Bellman-Ford.[83] For reference, the computational complexity of the classical Dijkstra's algorithm is $\mathcal{O}(|\boldsymbol{v}|^2)$ and Bellman-Ford is $\mathcal{O}(|\boldsymbol{v}||\boldsymbol{e}|)$. Note that these algorithms will find the shortest paths to all vertices in $\boldsymbol{v}$, and not just on $\boldsymbol{p}$, at once.

After finding $t^*(p,h)$ from all $h \in \boldsymbol{h}$, we compute the minimum travel time $t^*(p)$ to any hospital by comparing the different options each patient p has. Thus,

$$t^*(p) = \min_{h \in H} t^*(p,h) \tag{11}$$

In a pre-earthquake scenario, all hospitals will be functional; thus, Eq. 11 finds the shortest time to reach an acute care hospital p (Figure 8). In an earthquake, the number of functional hospitals can be reduced. Thus, we adjust Eq. 11 to

$$\overline{T^*(p)} = \min_{h \in \overline{H}} t^*(p,h) \tag{12}$$

where $\overline{\boldsymbol{h}} = \{h | B_h > 0 \quad \forall h \in \boldsymbol{h}\}$. Thus, $\overline{\boldsymbol{h}}$ is a set with a random selection of elements, i.e., hospital vertices. Eq. 12 couples the network model to the risk model because the condition of hospital h to be in $\overline{\boldsymbol{h}}$ is to have at least one functional bed. From Eq. 8, this condition implies that at least one building is functional. While this may be an optimistic condition, as some large campuses will need more than one building, we use it to showcase how to couple network models with risk models to assess post-earthquake healthcare access. Thus, $\overline{T^*(p)}$ is a random variable. We solve Eq. 12 using the 5,000 Monte Carlo simulations obtained before.

Bay Area's Transportation System

We study the entire San Francisco Bay, where the transportation network is massive, with $|\boldsymbol{v}|$ =1.5 million vertices and $|\boldsymbol{e}|$ = 2.8 million edges. The edges in the graph represent the roads in the

transportation system, whose information was obtained from the San Francisco Region Roadways[84] and OpenStreetMap (OSM).[85] We incorporated directional and travel time data into the network models using OSM's OSMnx library.[86] We couple the transportation network data to the hospital and the patient data. The 76 hospitals are embedded in the network models by identifying the network's vertices closest to the hospital locations, forming the set $\boldsymbol{h}$. In addition, we obtained population data at 1,613 zip codes. We assume the number of patients is proportional to the population. To form the set $\boldsymbol{p}$, we identify the network's vertices closest to the census tract's centroids (Figure 8).

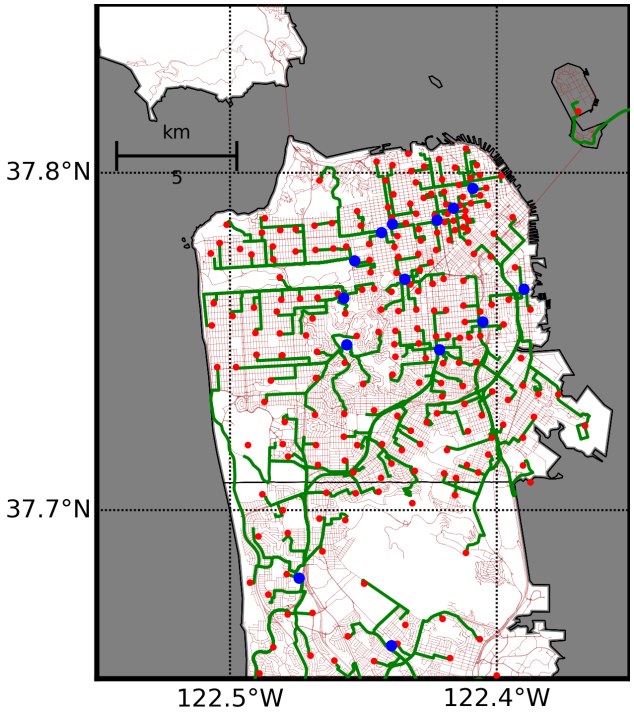

Figure 8: Shortest paths from patient vertices ($p \in \boldsymbol{p}$) to hospital vertices ($h \in \boldsymbol{h}$) before the earthquake in the San Francisco county. The transportation network is shown in brown lines, the shortest paths in green lines, hospital vertices in blue dots, and patient vertices in red dots.

Data Availability

The hospital data are publicly available in the California Department of Health Care Access and Information's Portal: `https://hcai.ca.gov/facilities/building-safety/facility-detail/`. The transportation data are publicly available in the San Francisco's Metropolitan Transportation Commission's Portal `https://opendata.mtc.ca.gov/`. In addition, we made the hospital disruption simulations and the pre-processed network data accessible in the following NSF's DesignSafe repository: `https://doi.org/10.17603/ds2-pc7z-7227`.

Code Availability

The risk model was run with NHERI SimCenter's R2D software, open and publicly available: `https://simcenter.designsafe-ci.org/research-tools/r2dtool/`. Also, we made the code to

run the network model coupled to the risk model publicly available in the following NSF's DesignSafe repository: `https://doi.org/10.17603/ds2-pc7z-7227`.

Acknowledgements

We thank the financial support of the New York University's Tandon School of Engineering for this research.

Competing Interests

The authors declare no competing interests.

Author's contributions

L.C. conceived and formulated the risk-network model. C.K., D.M., X.L., and J.W. compiled and pre-processed the hospital and transportation data. L.C., C.K., and A.Z. run the risk-network simulations. L.C. drafted the manuscript with contributions and editing from all the authors.

References

[1] Hariri-Ardebili, M. A. *et al.* A Perspective towards Multi-Hazard Resilient Systems: Natural Hazards and Pandemics. *Sustainability* **14**, 4508 (2022). URL https://www.mdpi.com/2071-1050/14/8/4508.

[2] Turkish Medical Association. Hatay Earthquakes Executive Summary of the First Month Evaluation Report. Turkish Medical Association. Tech. Rep. (2023). URL www.ttb.org.tr/userfiles/files/1ayraporu.pdf.

[3] Ceferino, L., Kiremidjian, A. & Deierlein, G. Probabilistic Model for Regional Multiseverity Casualty Estimation due to Building Damage Following an Earthquake. *ASCE-ASME Journal of Risk and Uncertainty in Engineering Systems, Part A: Civil Engineering* **4**, 04018023 (2018). URL http://ascelibrary.org/doi/10.1061/AJRUA6.0000972.

[4] Ceferino, L., Kiremidjian, A. & Deierlein, G. Regional Multiseverity Casualty Estimation Due to Building Damage following a Mw 8.8 Earthquake Scenario in Lima, Peru. *Earthquake Spectra* **34**, 1739–1761 (2018). URL http://journals.sagepub.com/doi/10.1193/080617EQS154M.

[5] Zhang, L., Li, H., Carlton, J. R. & Ursano, R. The injury profile after the 2008 earthquakes in China. *Injury* **40**, 84–86 (2009). URL https://linkinghub.elsevier.com/retrieve/pii/S0020138308003689.

[6] Fuse, A. *et al.* Onsite Medical Rounds and Fact-finding Activities Conducted by Nippon Medical School in Miyagi Prefecture after the Great East Japan Earthquake 2011. *Journal of Nippon Medical School* **78**, 401–404 (2011). URL http://www.jstage.jst.go.jp/article/jnms/78/6/78_6_401/_article.

[7] Suda, T. *et al.* Medical Needs in Minamisanriku Town after the Great East Japan Earthquake. *The Tohoku Journal of Experimental Medicine* **248**, 73–86 (2019). URL https://www.jstage.jst.go.jp/article/tjem/248/2/248_73/_article.

[8] Centers for Disease Control and Prevention (CDC). Post-earthquake injuries treated at a field hospital — Haiti, 2010. *MMWR. Morbidity and mortality weekly report* **59**, 1673–1677 (2011).

[9] Noh, H. Y., Kiremidjian, A., Ceferino, L. & So, E. Bayesian Updating of Earthquake Vulnerability Functions with Application to Mortality Rates. *Earthquake Spectra* **33**, 1173–1189 (2017).

[10] Dilsiz, A. *et al.* StEER: 2023 Mw 7.8 Kahramanmaras, Türkiye Earthquake Sequence Preliminary Virtual Reconnaissance Report (PVRR). Tech. Rep., Designsafe-CI (2023). URL https://www.designsafe-ci.org/data/browser/public/designsafe.storage.published/PRJ-3824v2/#details-942732811040452115-242ac11b-0001-012.

[11] Alisjahbana, I., Graur, A., Lo, I. & Kiremidjian, A. Optimizing strategies for post-disaster reconstruction of school systems. *Reliability Engineering and System Safety* **219**, 108253 (2022). URL https://doi.org/10.1016/j.ress.2021.108253. Publisher: Elsevier Ltd.

[12] Ghafory-Ashtiany, M. & Hosseini, M. Post-Bam earthquake: recovery and reconstruction. *Natural Hazards* **44**, 229–241 (2008). URL http://link.springer.com/10.1007/s11069-007-9108-3.

[13] California Seismic Safety Commission (CSSC). Findings and Recommendations on Hospital Seismic Safety. Tech. Rep. (2001).

[14] Cheevers, J. & Abrahamson, A. Earthquake: The Long Road Back : Hospitals Strained to the Limit by Injured : Medical care: Doctors treat quake victims in parking lots. Details of some disaster-related deaths are released. *Los Angeles Times* (1994). URL `https://www.latimes.com/archives/la-xpm-1994-01-19-me-13343-story.html`.

[15] Schultz, C. H., Koenig, K. L. & Lewis, R. J. Implications of hospital evacuation after the Northridge, California, earthquake. *New England Journal of Medicine* **348**, 1349–1355 (2003).

[16] Seismic Safety Commission State of California. Northridge Earthquake: Turning Loss to Gain. Tech. Rep. (1995).

[17] Meade, C. & Kulick, J. SB1953 and the Challenge of Hospital Seismic Safety in California. Tech. Rep., RAND Corporation (2007). Issue: January.

[18] California Health and Human Services. Hospital Building Data (2023). URL `https://data.chhs.ca.gov/dataset/hospital-building-data`.

[19] Preston, B. *et al. Updating the Costs of Compliance for California's Hospital Seismic Safety Standards* (RAND Corporation, 2019). URL `https://www.rand.org/pubs/research_reports/RR3059.html`. Publication Title: Updating the Costs of Compliance for California's Hospital Seismic Safety Standards.

[20] Yavari, S., Chang, S. E. & Elwood, K. J. Modeling Post-Earthquake Functionality of Regional Health Care Facilities **26**, 869–892 (2010).

[21] Jacques, C. C. *et al.* Resilience of the canterbury hospital system to the 2011 Christchurch earthquake. *Earthquake Spectra* **30**, 533–554 (2014). ISBN: 8755-2930.

[22] Tarque, N. *et al.* Basic Seismic Response Capability of Hospitals in Lima, Peru. *Disaster Medicine and Public Health Preparedness* 1–6 (2018).

[23] Hassan, E. M. & Mahmoud, H. Full functionality and recovery assessment framework for a hospital subjected to a scenario earthquake event. *Engineering Structures* **188**, 165–177 (2019). URL `https://linkinghub.elsevier.com/retrieve/pii/S0141029617338440`.

[24] Merino-Peña, Y., Ceferino, L., Pizarro, S. & De La Llera, J. C. Modeling Hospital Resources based on Global Epidemiology after Earthquake-related Disasters. preprint (2023). URL `https://engrxiv.org/preprint/view/3238/version/4552`.

[25] Yi, P., George, S. K., Paul, J. A. & Lin, L. Hospital capacity planning for disaster emergency management. *Socio-Economic Planning Sciences* **44**, 151–160 (2010). URL `http://dx.doi.org/10.1016/j.seps.2009.11.002`. Publisher: Elsevier Ltd.

[26] Gul, M. & Guneri, A. F. A comprehensive review of emergency department simulation applications for normal and disaster conditions. *Computers and Industrial Engineering* **83**, 327–344 (2015). URL `http://dx.doi.org/10.1016/j.cie.2015.02.018`. Publisher: Elsevier Ltd ISBN: 9021238330.

[27] Aghapour, A. H., Yazdani, M., Jolai, F. & Mojtahedi, M. Capacity planning and reconfiguration for disaster-resilient health infrastructure. *Journal of Building Engineering* **26**, 100853 (2019). URL https://doi.org/10.1016/j.jobe.2019.100853. Publisher: Elsevier Ltd.

[28] Ardagh, M. W. *et al.* The initial health-system response to the earthquake in Christchurch, New Zealand, in February, 2011. *The Lancet* **379**, 2109–2115 (2012). URL http://dx.doi.org/10.1016/S0140-6736(12)60313-4. Publisher: Elsevier Ltd ISBN: 1474-547X (Electronic)\r0140-6736 (Linking).

[29] Kirsch, T. D. *et al.* Impact on hospital functions following the 2010 Chilean earthquake. *Disaster medicine and public health preparedness* **4**, 122–128 (2010). ArXiv: 1011.1669v3 ISBN: 1938-744X (Electronic)\r1935-7893 (Linking).

[30] Shimoto, M. *et al.* Hospital Evacuation Implications After the 2016 Kumamoto Earthquake. *Disaster Medicine and Public Health Preparedness* **16**, 2680–2682 (2022). URL https://www.cambridge.org/core/product/identifier/S1935789322000258/type/journal_article.

[31] Achour, N. & Miyajima, M. Post-earthquake hospital functionality evaluation: The case of Kumamoto Earthquake 2016. *Earthquake Spectra* **36**, 1670–1694 (2020). URL http://journals.sagepub.com/doi/10.1177/8755293020926180.

[32] Naghi, T. *et al.* Musculoskeletal injuries associated with earthquake: A report of injuries of Iran's December 26, 2003 Bam earthquake casualties managed in tertiary referral centers. *Injury* **36**, 27–32 (2005). ISBN: 0020-1383 (Print)\n0020-1383 (Linking).

[33] Gök, M. & Melik, M. A. Clinical features and outcomes of orthopaedic injuries after the kahramanmaraş earthquake: a retrospective study from a hospital located in the affected region. *Scandinavian Journal of Trauma, Resuscitation and Emergency Medicine* **32**, 10 (2024). URL https://sjtrem.biomedcentral.com/articles/10.1186/s13049-024-01181-6.

[34] European Resuscitation Council. Part 12: From Science to Survival: Strengthening the Chain of Survival in Every Community. *Circulation* **102** (2000). URL https://www.ahajournals.org/doi/10.1161/circ.102.suppl_1.I-358.

[35] Ceferino, L., Merino, Y., Pizarro, S., Moya, L. & Ozturk, B. Toward Engineering the Earthquake Response and the Survival Chain. *(In Review)* .

[36] American Red Cross Multi-Disciplinary Team. Report on the 2010 Chilean Earthquake and Tsunami Response: U.S. Geological Survey Open-File Report 2011-1053 v1.1. Tech. Rep., United States Geological Survey & American Red Cross, Virginia (2011). URL https://pubs.usgs.gov/of/2011/1053/. ISBN: 9781621002918.

[37] Ceferino, L., Mitrani-Reiser, J., Kiremidjian, A., Deierlein, G. & Bambarén, C. Effective plans for hospital system response to earthquake emergencies. *Nature Communications* **11**, 4325 (2020). URL http://dx.doi.org/10.1038/s41467-020-18072-w. Publisher: Springer US.

[38] Hassan, E. M. & Mahmoud, H. N. Orchestrating performance of healthcare networks subjected to the compound events of natural disasters and pandemic. *Nature Communications* **12**, 1–12 (2021). URL http://dx.doi.org/10.1038/s41467-021-21581-x. Publisher: Springer US.

[39] Rambha, T., Nozick, L. K., Davidson, R., Yi, W. & Yang, K. A stochastic optimization model for staged hospital evacuation during hurricanes. *Transportation Research Part E* **151**, 102321 (2021). URL https://doi.org/10.1016/j.tre.2021.102321. Publisher: Elsevier Ltd.

[40] Department of Health Care Access and Information. Facility Detail (2013). URL https://hcai.ca.gov/construction-finance/facility-detail/.

[41] Ceferino, L. *et al.* Combining Seismic Risk Analysis and Network Modeling to Assess Hospital Service Accessibility in the Bay Area, California. In *The 14th International Conference on Application of Statistics and Probability in Civil Egnineering* (Dublin, Ireland, 2023).

[42] Department of Health Care Access and Information. Seismic Performance Ratings (2023). URL https://hcai.ca.gov/construction-finance/seismic-compliance-and-safety/seismic-performance-ratings/.

[43] American Society of Civil Engineers (ASCE). Minimum Design Loads and Buildings and Other Structures (ASCE/SEI 7-16). Tech. Rep., American Society of Civil Engineers (2017). ISBN: 9780784414248.

[44] California Department of Health Care Access and Information (HCAI). Changes to Seismic Safety Law (2023). URL https://hcai.ca.gov/construction-finance/seismic-compliance-and-safety/seismic-legislation/#HFSA.

[45] Detweiler, S. T. & Wein, A. The HayWired earthquake scenario—Earthquake hazards. U.S. Geological Survey Scientific Investigations Report 2017–5013–A–H (2018). Series: Scientific Investigations Report.

[46] Jacques, C. C. Resilience of Healthcare in Disasters: A Systems Approach (2016).

[47] Miller, M. & Baker, J. W. Coupling mode-destination accessibility with seismic risk assessment to identify at-risk communities. *Reliability Engineering & System Safety* **147**, 60–71 (2016). URL http://dx.doi.org/10.1016/j.ress.2015.10.018. Publisher: Elsevier.

[48] Porter, K. An Overview of PEER's Performance-Based Earthquake Engineering Methodology. In *Ninth International Conference on Applications of Statistics and Probability in Civil Engineering (ICASP9)* (San Francisco, 2003).

[49] Moehle, J. & Deierlein, G. G. A framework methodology for performance-based earthquake engineering. *Proceedings of the 13 th World Conference on Earthquake Engineering* 3812–3814 (2004).

[50] Krawinkler, H. & Miranda, E. Preformance -based Earthquake Engineering. In *Earthquake Engineering: From Engineering Seismology to Performance-Based Engineering* (CRC Press, Boca Raton, 2004), first edn.

[51] Lee, R. & Kiremidjian, A. S. Uncertainty and correlation for loss assessment of spatially distributed systems. *Earthquake Spectra* **23**, 753–770 (2007).

[52] Lin, P., Wang, N. & Ellingwood, B. R. A risk de-aggregation framework that relates community resilience goals to building performance objectivess. *Sustainable and Resilient Infrastructure* **1**, 1–13 (2016). URL https://www.tandfonline.com/doi/full/10.1080/23789689.2016.1178559.

[53] Heresi, P. & Miranda, E. Structure-to-structure damage correlation for scenario-based regional seismic risk assessment. *Structural Safety* **95**, 102155 (2022). URL https://doi.org/10.1016/j.strusafe.2021.102155. Publisher: Elsevier Ltd.

[54] Wang, C. & Ellingwood, B. R. Discussion: "Structure-to-structure damage correlation for scenario-based regional seismic risk assessment" by P. Heresi and E. Miranda [Structural Safety 95 (2022) 102155]. *Structural Safety* **97**, 102203 (2022). URL https://linkinghub.elsevier.com/retrieve/pii/S0167473022000182.

[55] Heresi, P. & Miranda, E. RPBEE: Performance-based earthquake engineering on a regional scale. *Earthquake Spectra* 87552930231179491 (2023). URL http://journals.sagepub.com/doi/10.1177/87552930231179491.

[56] Goda, K. & Hong, H. P. Estimation of Seismic Loss for Spatially Distributed Buildings. *Earthquake Spectra* **24**, 889–910 (2008). URL http://earthquakespectra.org/doi/abs/10.1193/1.2983654.

[57] Goda, K. & Hong, H. P. Spatial correlation of peak ground motions and response spectra. *Bulletin of the Seismological Society of America* **98**, 354–365 (2008). ISBN: 0037-1106.

[58] Loth, C. & Baker, J. W. A spatial cross-correlation model of spectral accelerations at multiple periods. *Earthquake Engineering & Structural Dynamics* **41**, 397–417 (2013). URL http://onlinelibrary.wiley.com/doi/10.1002/eqe.2230/full. ISBN: 1096-9845.

[59] Markhvida, M., Ceferino, L. & Baker, J. W. Modeling spatially correlated spectral accelerations at multiple periods using principal component analysis and geostatistics. *Earthquake Engineering & Structural Dynamics* **47**, 1107–1123 (2018). URL https://onlinelibrary.wiley.com/doi/10.1002/eqe.3007.

[60] Markhvida, M., Walsh, B., Hallegatte, S. & Baker, J. Quantification of disaster impacts through household well-being losses. *Nature Sustainability* **3**, 538–547 (2020). URL http://dx.doi.org/10.1038/s41893-020-0508-7. Publisher: Springer US.

[61] Dhulipala, S. L., Burton, H. V. & Baroud, H. A Markov framework for generalized post-event systems recovery modeling: From single to multihazards. *Structural Safety* **91**, 102091 (2021). URL https://linkinghub.elsevier.com/retrieve/pii/S0167473021000175.

[62] Hulsey, A. M., Baker, J. W. & Deierlein, G. G. High-resolution post-earthquake recovery simulation: Impact of safety cordons. *Earthquake Spectra* **38**, 2061–2087 (2022). URL http://journals.sagepub.com/doi/10.1177/87552930221075364.

[63] Du, A., Wang, X., Xie, Y. & Dong, Y. Regional seismic risk and resilience assessment: Methodological development, applicability, and future research needs – An earthquake engineering perspective. *Reliability Engineering & System Safety* **233**, 109104 (2023). URL https://linkinghub.elsevier.com/retrieve/pii/S0951832023000194.

[64] Mitrani-Reiser, J. *et al.* A Functional Loss Assessment of a Hospital System in the Bío-Bío Province. *Earthquake Spectra* **28**, 473–502 (2012).

[65] Jayaram, N. & Baker, J. W. Statistical tests of the joint distribution of spectral acceleration values. *Bulletin of the Seismological Society of America* **98**, 2231–2243 (2008). ISBN: 10.1785/0120070208.

[66] McKenna, F. *et al.* NHERI-SimCenter/R2DTool: Version 2.1.0 (2022). URL `https://zenodo.org/record/6404528`.

[67] Deierlein, G. G. *et al.* A Cloud-Enabled Application Framework for Simulating Regional-Scale Impacts of Natural Hazards on the Built Environment. *Frontiers in Built Environment* **6**, 1–18 (2020).

[68] Deierlein, G. G. & Adam Zsarnóczay, e. State of the Art in Computational Simulation for Natural Hazards Engineering. Tech. Rep., [object Object] (2021). URL `https://zenodo.org/record/2579581`. Version Number: v2.

[69] Field, E. H. *et al.* Uniform California earthquake rupture forecast, version 2 (UCERF 2). *Bulletin of the Seismological Society of America* **99**, 2053–2107 (2009). ISBN: 0037-1106.

[70] Thompson, E. M., Wald, D. J. & Worden, C. B. A VS30 Map for California with Geologic and Topographic Constraints. *Bulletin of the Seismological Society of America* **104**, 2313–2321 (2014). URL `https://pubs.geoscienceworld.org/bssa/article/104/5/2313-2321/351481`.

[71] Abrahamson, N. A., Silva, W. J. & Kamai, R. Summary of the ASK14 Ground Motion Relation for Active Crustal Regions. *Earthquake Spectra* **30**, 1025–1055 (2014). URL `http://journals.sagepub.com/doi/10.1193/070913EQS198M`. ISBN: 2012120717.

[72] Douglas, J. & Edwards, B. Recent and future developments in earthquake ground motion estimation. *Earth-Science Reviews* **160**, 203–219 (2016). URL `https://linkinghub.elsevier.com/retrieve/pii/S0012825216301672`.

[73] Jayaram, N. & Baker, J. W. Correlation model for spatially distributed ground-motion intensities. *Earthquake Engineering & Structural Dynamics* **38**, 1687–1708 (2009). ISBN: 1096-9845.

[74] Markhvida, M., Ceferino, L. & Baker, J. Effect of ground motion correlation on regional seismic loss estimation : application to Lima , Peru using a cross-correlated principal component analysis model. In *12th International Conference on Structural Safety and Reliability*, 1844–1853 (Vienna, Austria, 2017).

[75] Lallemant, D., Kiremidjian, A. & Burton, H. Statistical procedures for developing earthquake damage fragility curves: STATISTICAL PROCEDURES FOR DAMAGE FRAGILITY CURVES. *Earthquake Engineering & Structural Dynamics* **44**, 1373–1389 (2015). URL `https://onlinelibrary.wiley.com/doi/10.1002/eqe.2522`.

[76] Federal Emergency Management Agency (FEMA). Hazus Earthquake Model, Technical Manual (Hazus 4.2 SP3). Tech. Rep., Federal Emergency Management Agency, Washington, DC (2020). Issue: October.

[77] Zsarnóczay, A. & Deierlein, G. G. Pelicun – A Computational Framework for Estimating Damage, Loss, and Community Resilience. In *The 17th World Conference on Earthquake Engineering* (Sendai, Japan, 2020).

[78] American Society of Civil Engineers (ASCE). *Seismic Evaluation and Retrofit of Existing Buildings (ASCE/SEI 41-17)* (American Society of Civil Engineers, 2017).

[79] Kircher, C. a. Earthquake Loss Estimation Methods for Welded Steel Moment-Frame Buildings. *Earthquake Spectra* **19**, 365–384 (2003). URL `http://earthquakespectra.org/doi/abs/10.1193/1.1572171`.

[80] California Building Standards Commission. *California Building Standards Code* (International Code Council, 2022).

[81] Federal Emergency Management Agency (FEMA). Building Codes Save: A Nationwide Study. Losses Avoided as a Result of Adoption Hazard-Resistant Building Codes. Tech. Rep., FEMA, Washington, DC (2020). Issue: November.

[82] Deierlein, G. & Zsarnóczay, A. State of the Art in Computational Simulation for Natural Hazards Engineering. *NHERI SimCenter* (2021). URL `http://doi.org/10.5281/zenodo.4558106`.

[83] Bondy, J. A. & Murty, U. S. R. *Graph theory with applications* (North Holland, New York, 1976).

[84] Association of Bay Area Governments. San Francisco Bay Region Roadways (2021). URL `https://opendata.mtc.ca.gov/datasets/cc308da7798a4b03926e22c1f815d553_0/explore?location=37.838399%2C-122.367566%2C8.73`.

[85] OpenStreetMap Contributors. Planet dump [Data file from 12/2023]. URL `https://planet.openstreetmap.org`.

[86] Boeing, G. OSMnx: New methods for acquiring, constructing, analyzing, and visualizing complex street networks. *Computers, Environment and Urban Systems* **65**, 126–139 (2017). URL `https://linkinghub.elsevier.com/retrieve/pii/S0198971516303970`.